2019 International Conference on Robotics and Automation (ICRA)
Palais des congres de Montreal, Montreal, Canada, May 20-24, 2019

A Clustering Approach to Categorizing 7 Degree-of-Freedom Arm Motions during Activities of Daily Living

Yuri Gloumakov, Adam J. Spiers, *Member, IEEE*, and Aaron M. Dollar, *Senior Member, IEEE*

***Abstract*— In this paper we present a novel method of categorizing naturalistic human arm motions during activities of daily living using clustering techniques. While many current approaches attempt to define all arm motions using heuristic interpretation, or a combination of several abstract motion primitives, our unsupervised approach generates a hierarchical description of natural human motion with well recognized groups. Reliable recommendation of a subset of motions for task achievement is beneficial to various fields, such as robotic and semi-autonomous prosthetic device applications. The proposed method makes use of well-known techniques such as dynamic time warping (DTW) to obtain a divergence measure between motion segments, DTW barycenter averaging (DBA) to get a motion average, and Ward's distance criterion to build the hierarchical tree. The clusters that emerge summarize the variety of recorded motions into the following general tasks: reach-to-front, transfer-box, drinking from vessel, on-table motion, turning a key or door knob, and reach-to-back pocket. The clustering methodology is justified by comparing against an alternative measure of divergence using Bezier coefficients and K-medoids clustering.**

I. Introduction

The human arm is a remarkable tool that affords us the ability to accomplish complex manipulation tasks. Unlike the study of the lower limbs with regard to gait, the arm has much more varied patterns of motions that it regularly performs [1]. Despite this, humans consistently perform various reaching, grasping, and manipulation tasks in a predictable pattern [2] without much cognitive burden. Since there exists some apparent regularity of human motion patterns, it is predicted that a simplified motion model can be found, for example, by extracting a subset of representative movements. We investigate a data driven clustering approach to identify natural groupings of the 7 degree-of-freedom (DOF) joint angle trajectories of the upper-limb (hereafter simply referred to as "arm motion") obtained from individuals performing a range of selected activities of daily living (ADLs).

Clustering sub-motions, instead of the entire task motion trajectory, is useful in a variety of domains, such as controlling the functionality of a semi-autonomous prosthetic device by using sub-motions to recreate a larger set of possible tasks. Research groups investigating joint synergies to control active prosthetic wrists or elbows have primarily focused on reaching motions [3], [4]. While our methodology is not limited to only this application, the development of an arm motion hierarchy formalizes the stratification of reaching and manipulation. This enables future efforts to focus on consistent and verifiable clusters of motions.

This work was supported by the Congressionally-Directed Medical Research Programs (CDMRP) under grant- W81XWH-15-10407.

Y. Gloumakov and A.M. Dollar are with the Mechanical Engineering and Materials Science Department, Yale University, New Haven, CT 06511 USA, (email: {yuri.gloumakov, aaron.dollar} @yale.edu). A.J. Spiers is with the Max Planck Institute for Intelligent Systems, Stuttgart, 70597, Germany (email: a.spiers@is.mpg.de)

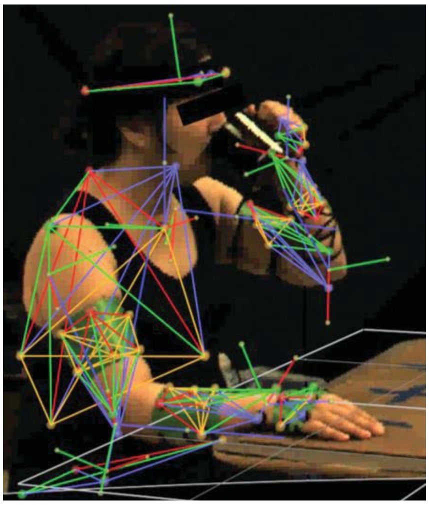

Figure 1. Subject performing an ADL task, drinking from a mug. The subject's motion capture 'skeleton' is superimposed in this image. Redundant markers are included to enable the prediction of occluded marker locations and maintain the ability to identify joint centers.

Out of the infinitum of motions that the human arm can achieve, we looked to only use the most useful ones across individuals, i.e. most common ADLs, as the set of motions to cluster (Fig. 1). For the tasks we asked our subjects to perform in this work (Table 1), we selected ones largely inspired by the standardized 'outcome measure' arm function assessment tools of AM-ULA [5] and various surveys that queried motion-impaired participants on common tasks that they find difficult [6]–[8]. These tasks generally relate to hygiene, grooming, dressing, food preparation, and eating, and are crucial for independent living.

Past research on upper limb motion has spanned a variety of fields with different research groups exploring various techniques to extract insight into how humans control and make use of their upper limbs. Such research has covered non-linear control, neural networks, and musculoskeletal modelling [9]. Some groups have also attempted to identify and make use of underlying healthy motion patterns to control upper-limb prosthetic devices. These investigations

978-1-5386-6027-0/19/$31.00 ©2019 IEEE

include using artificial neural networks to predict or discriminate upper-limb functions [4], [10] or performing pattern recognition of simultaneous motion primitives [11] in healthy subjects. Another group examined healthy participants performing various ADL tasks and extracted a subset of motion primitives using functional principal component analysis (fPCA) [12]. A much more straight forward approach to controlling an upper-limb device could instead focus on clusters of sequential sub-motions that recreate the complete task. On-line motion recognition, as well as a hierarchical description of non-ADL motion segments has been performed in [13]. However, the focus was on automatic motion recognition of the whole body rather than on sequential motion segments and results were not deterministic. Other related fields include rehabilitation efforts, which have investigated motion patterns of healthy participants by identifying only the ranges of joint angles [14], [15]. Therefore, although some groups have attempted to extract underlying simplified motion patterns [4], [11]–[13], none have used a clustering approach that stratifies arm motions related to ADLs.

For the remainder of this paper, we begin with a description of our experimental protocol (section II), describe our analytical methodology and the results of its application (section III), and then we include a discussion of the results (section IV). We finish with a conclusion and future work (section V).

II. Experimental Protocol

A. Task Protocol

The set of motions that are used in this study were collected from healthy individuals performing tasks that generally occur during daily life. The tasks used in the study, which were based on the standard functional measure AM-ULA [5], are listed in Table 1 with the setup described in more detail in Fig. 2. We only included a subset of tasks found in AM-ULA that were easy to segment into sub-motions, which is important for analyzing distinct motion segments related to ADLs rather than an entire complex motion that occurs during a task. For example, the task of drinking from a cup may involve clear segments of reaching, grasping, bringing to the mouth, and returning to a table. Tasks such as folding a towel or putting on a shirt were omitted from the protocol due to lack of distinct motion segments. Despite including some reaching and transferring components, cyclical tasks, such as cutting with a knife or stirring, were also omitted due to the difficulty in deciding the start and end points of a motion segment. Although a set of feature variables could potentially be used to represent cyclical tasks, such as wavelet transform or discrete Fourier transform [16], these representation methods would not be appropriate for the motions we have considered thus far.

The protocol was completed by 5 subjects (3 male, 2 female) who performed the 24 tasks 3 times each, to provide a way to average or smooth motions during analysis as well as to account for outliers. Each task was segmented into 2 to 6 distinct sub-motions, totaling to 86 motion segments per person. Each participant performed the protocol over the course of 5 hours in a single visit. They were instructed to start and end each task in specified 'rest poses', i.e. standing with hands by their sides or sitting with palms on a table surface. Minimal additional instruction were given on how to perform the task.

Table 1. Each tasks is segmented according to the description below. The task code is used in the results section. Unless otherwise specified, standing tasks started and ended with the subjects' hands by their side while for sitting tasks the hands were to start and end on the table palm side down. The height of the table is 74 cm, and is elevated to 92 cm to simulate a counter top for the standing cup and mug tasks. The mug (9.5 cm height, 8 cm diameter), can (7.5 cm height, cm diameter), box (21x37x19 cm), and suitcase (43x9x30 cm) weigh 0.36, 0.09, 0.23, and 1.36 kg respectively. The shelves are 80, 140, and 180 cm above the floor. Door knob and handle are 90 cm above the floor, and the simulated door swivels with an 84 cm radius.

Task Code	Standing tasks
t2b	(1) reach for box on the top shelf (2) move box to bottom shelf (3) return hands
b2t	(1) reach for box on the bottom shelf (2) move box to top shelf (3) return hands
t2m	(1) reach for box on the top shelf (2) move box to middle shelf (3) return hands
m2t	(1) reach for box on the middle shelf (2) move box to top shelf (3) return hands
m2b	(1) reach for box on the middle shelf (2) move box to bottom shelf (3) return hands
b2m	(1) reach for box on the bottom shelf (2) move box to middle shelf (3) return hands
ke	(1) bring key to hole (2) insert key (3) turn key (4) turn back (5) remove key and return hand
kn	(1) reach for door knob (2) turn knob (3) turn back (4) return hand
dh	(1) reach for door handle (2) turn handle (3) open door (4) return hand
oh	(1) reach for can on top shelf (2) bring can down in front of the body
mp	(1) reach for mug in location C1 (2) take a sip (3) return mug (4) return hand
md	(1) reach for mug in location C2 (2) take a sip (3) return mug (4) return hand
mc	(1) reach for mug in location C3 (2) take a sip (3) return mug (4) return hand
cp	(1) reach for cup in location C1 (2) take a sip (3) return mug (4) return hand
cd	(1) reach for cup in location C2 (2) take a sip (3) return mug (4) return hand
cc	(1) reach for cup in location C3 (2) take a sip (3) return mug (4) return hand
st	(1) reach for suitcase (2) transfer suitcase to table (3) return hands
ax	(1) bring hand to contralateral axilla (2) return hand
pt	(1) bring hand to back pocket (2) return hand
	Sitting tasks
sp	(1) reach for spoon (2) bring spoon to bowl (3) scoop (4) bring to mouth (5) return spoon (6) return hand
fr	(1) reach for fork (2) stab the middle of the plate (3) bring to mouth (4) return fork (5) return hand
ms	(1) reach for mug (2) take a sip (3) return mug (4) return hand
cs	(1) reach for cup (2) take a sip (3) return cup (4) return hand
pr	(1) reach for cup (2) pour into another cup (3) return cup (4) return hand

This study protocol was approved by Yale University Institutional Review Board, HSC# 1610018511.

B. Data Acquisition

Motions were recorded with a Vicon Motion Capture System (Oxford Metrics Limited, Oxford) using 12 infrared 'Bonita' model cameras, 1 video reference camera (synchronized with the Vicon system), and 55 body-worn

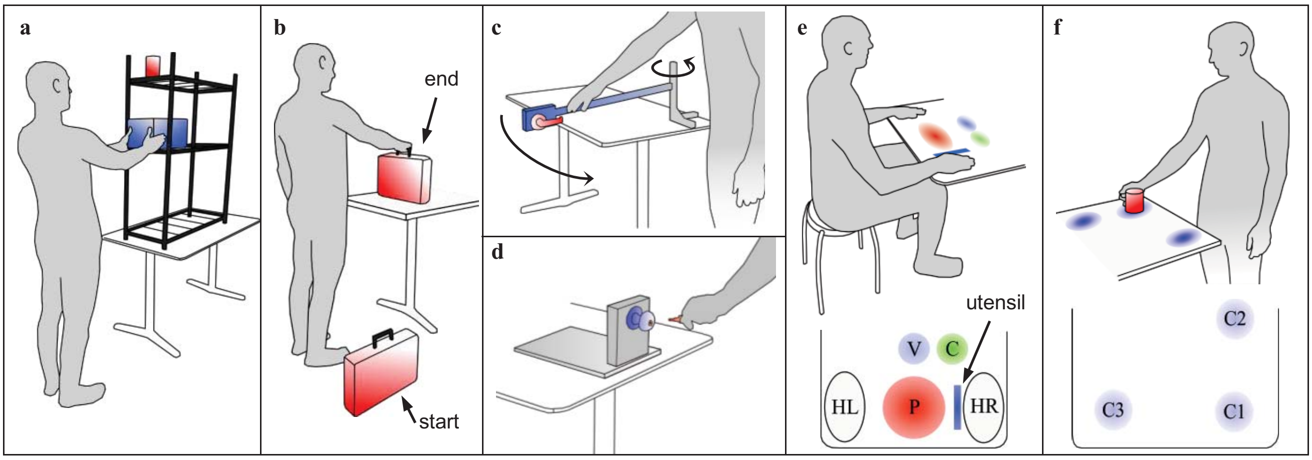

Figure 3. Depictions of several selected protocol tasks: (a) a box object was to be moved from one specified shelf to another, and the object on the top shelf is the location of the can during overhead reaching tasks, (b) the initial and final locations of the suitcase tasks, (c) simulated door opening task, and (d) simulated door knob and key tasks. (e) depicts the set up for the sitting tasks: the left and right hand start and end in HL and HR, a utensil is placed next to HR, a bowl or plate are placed in P, a cup or mug is placed in C, and a container to collect the water during the pouring task is placed in V. (f) depicts the three target locations of the standing cup and mug tasks, during which the table is elevated to simulate a countertop, where C2 is 25 cm from C1 and C3 is 45 cm from C1. The task conditions for left handed participants are mirrored.

reflective markers at a rate of 100 frames/second. Synchronized video from the reference camera was used to aid in marker identification in the Vicon Nexus software.

III. Data Analysis

The goal of the data analysis was to find how arm motions related to ADL cluster and what sort of groupings emerge. The collected data was first processed in the segmentation step in which each task (which is recorded as a separate motion capture file) is manually broken down into sequential reaching and manipulation joint angle trajectories. The sub-motions from each type of task and movement are then averaged to remove outliers. A divergence measure is chosen such that it reliably computes a similarity measure between motion segments, which are followed by a clustering step. The clustering result is then evaluated using multiple methods; observing the inter-cluster and intra-cluster variabilities, and quantifying the quality of the chosen divergence measure and clustering algorithm against an alternative set of divergence and clustering methods.

A. Motion Representation

Human arm time-series motion data can been described in various ways, such as using Cartesian coordinates of the humerus, forearm, and hand or joint angles obtained from the shoulder, elbow, and wrist. The joint angle method suffers from the fact that proximal DOF will have a different impact on the end effector trajectory during motion reconstruction or down sampling. However, fewer variables are required to reconstruct the upper-limb using joint angle definitions, which is an important factor when calculating the similarity between motions.

The arm angle model used in this paper is based on 7 DOF shoulder-elbow-wrist definitions described in [17] and is detailed in Fig. 3. The shoulder angles consist of (1) plane of elevation, (2) angle of elevation [18], (3) and internal axial rotation, using the second option for the humerus coordinate system in [17]. The (4) elbow angle is considered between

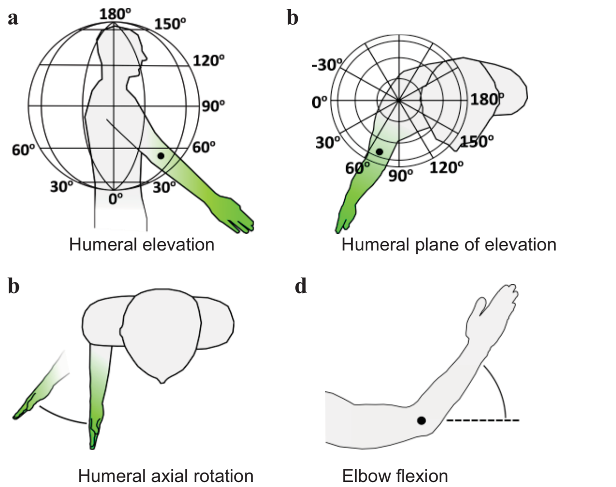

Figure 2. A sample of arm angle definitions. (a) Humeral elevation and (b) plane of elevation are depicted using the globe system described in [15]. (c) The elbow is positioned below the shoulder in the image to depict humeral axial rotation. (d) Elbow flexion. Wrist supination, flexion, and ulnar deviation are not depicted.

the forearm and humerus, while wrist angles consist of (5) supination, (6) wrist flexion, (7) and hand deviation.

B. Motion Segmentation

Arm motions during ADLs, whether reaching or manipulating an object, can be seen as a composite of individual sub-motions with which generalized tasks, such as drinking from a cup, are accomplished. Quantitative approaches to segmentation include derivative or zero velocity threshold [19], principle component analysis (PCA) [20], or a hybrid Hidden Markov Model (HMM) and PCA approach [21]. Despite advances in the field, verification of the segmentation algorithms were generally performed by comparing to a heuristically defined ground truth. Therefore, for the purposes of the present work, we segmented the motions manually each time the end effector reached zero velocity; when the participant made contact with, transferred, or returned the object, completed the task, or returned the hand back to its 'rest pose', detailed in Table 1.

C. Divergence Measure

Obtaining a divergence between time-series data requires that the data, or the corresponding feature vectors, be of equal length. While resampling or modeling time-series data frequently leads to a loss of some information, dynamic time warping (DTW) does not [22]. DTW works by replicating the frames between two time-series such that it creates a closer match between them while simultaneously making them equal in length. A divergence is calculated by summing the distances between each pairs of points of the two trajectories. In order to capture the divergence between arm motions that might be moving in opposite directions, such as bringing a cup to the mouth and returning the cup back to the table, DTW between each pair of motions was calculated twice: once with the original motion data, and once with one of the motions going in reverse. The smaller of the two divergence values is saved and used during the clustering step.

D. Averaging Motions

Due to task repetition and multiple participants, an average for the same sub-motions from the same task across all individuals was computed prior to clustering. Each average included 15 motion segments, three from each participant. Averaging also had a beneficial effect of minimizing the impact of noise and outliers; hierarchical clustering is particularly sensitive to it. A time-series average can be obtained in a variety of ways, one of which is linearly resampling all the data to the same length and taking a frame by frame average. This approach is sensitive to phase shift, so instead we used a DTW barycenter averaging (DBA) algorithm [23]. DBA uses an iterative approach where DTW is used to calculate the association of each frame of all motion segments to a consensus (average) segment, and a weighted average of the associated frames is calculated to obtain a new consensus frame. This is repeated for each frame of the consensus segment, and the process stops once no new associations are made. The initialization of the consensus segment does not impact the final average motion, and was initialized as one of the segments in the category.

E. Agglomerative Hierarchical Clustering

An effective clustering algorithm will be able to minimize variation within clusters while maximizing the difference between clusters, while also describing the overall structure of motions. Agglomerative hierarchical clustering [24] provides an easily interpretable dendrogram depicting how clusters are formed and their relationship to one another without requiring a predefined number of desired groupings. It works by successively merging individual motions based on the shortest specified pairwise divergence into a single cluster until one cluster containing all of the data is left. Ward's distance measure, is preferable for this application as it creates distinct clusters by accounting for both the within and cumulative cluster variances,

$$D = SS_{12} - (SS_1 + SS_2) \tag{1}$$

Where SS_1 and SS_2 are the sum of squares of each of the members of the cluster to its respective centroid, and SS_{12} is the sum of squares of the combined cluster. D is the calculated distance value. This computation is performed for each subsequent cluster without the need to identify the center of the clusters directly.

An alternative to agglomerative hierarchical clustering is a divisive algorithm; it starts out with all data belonging to the same cluster and iteratively splits a cluster in two based on the largest specified distance measure. An agglomerative approach is adopted due to the assumption that different motions do not belong to the same cluster but preferably are grouped sequentially, and by successfully merging them we hope to obtain an emerging pattern. One of the downsides to using this algorithm is its inability to adjust once a merge decision has been executed [25]. Thus, as described in Section D, we hope outlier effects were mitigated by averaging the same types of motions prior to clustering.

A set number of clusters are extracted from the hierarchical cluster tree using a straight-line cut, sliding the cut from the bottom to the top until six clusters are identified (Fig. 4). This seemed to be a good number of groupings based on heuristics, but, as will be discussed, other types of cuts are appropriate as well.

F. Cluster Quality

Evaluation of the emergent clusters is made by observing the inter-cluster and intra-cluster variabilities. These criteria identify how close clusters are to one another as well as the range of each cluster, respectively. These calculations compare individual motions from each person, rather than the average motion used during the clustering step. Results are summarized in Table 2.

Table 2. The nearest two motions belonging to different clusters and the farthest two motions within the same cluster are summarized. "Cluster #" indicates which cluster the motions belong to. The first column of motions belong to the cluster under examination, while the second column is the motion from the nearest cluster or the same cluster for the farthest case. The motion codes follow the format [subject ID: motion type].

	Cluster #	First Cluster	
Nearest	1-2	2: pt-2	2: dh-4
	2-4	2: dh-4	2: fr-5
	3-4	5: ke-2	1: fr-1
	4-3	1: fr-1	5: ke-2
	5-4	5: cs-3	4: pr-4
	6-2	3: t2m-2	3: oh-2
Farthest	1	3: pt-1	4: pt-1
	2	4: dh-3	5: dh-4
	3	5: ke-2	2: ke-4
	4	4: pr-2	2: sp-5
	5	3: mc-3	5: md-3
	6	4: b2t-2	2: t2b-2

Comparison of the clustering algorithm to alternative approaches is made using an original evaluation metric. Given that subjects performed each task three times, we expect that the repeated motion segments from the same subject would cluster together if motions were not previously averaged. By computing the hierarchical clustering tree using the individual motions, rather than the average of each motion type, we can compute an evaluation score. The score is calculated by identifying how often a motion segment is clustered with other motion segments of the same type from the same individual. For every pair of the same motion

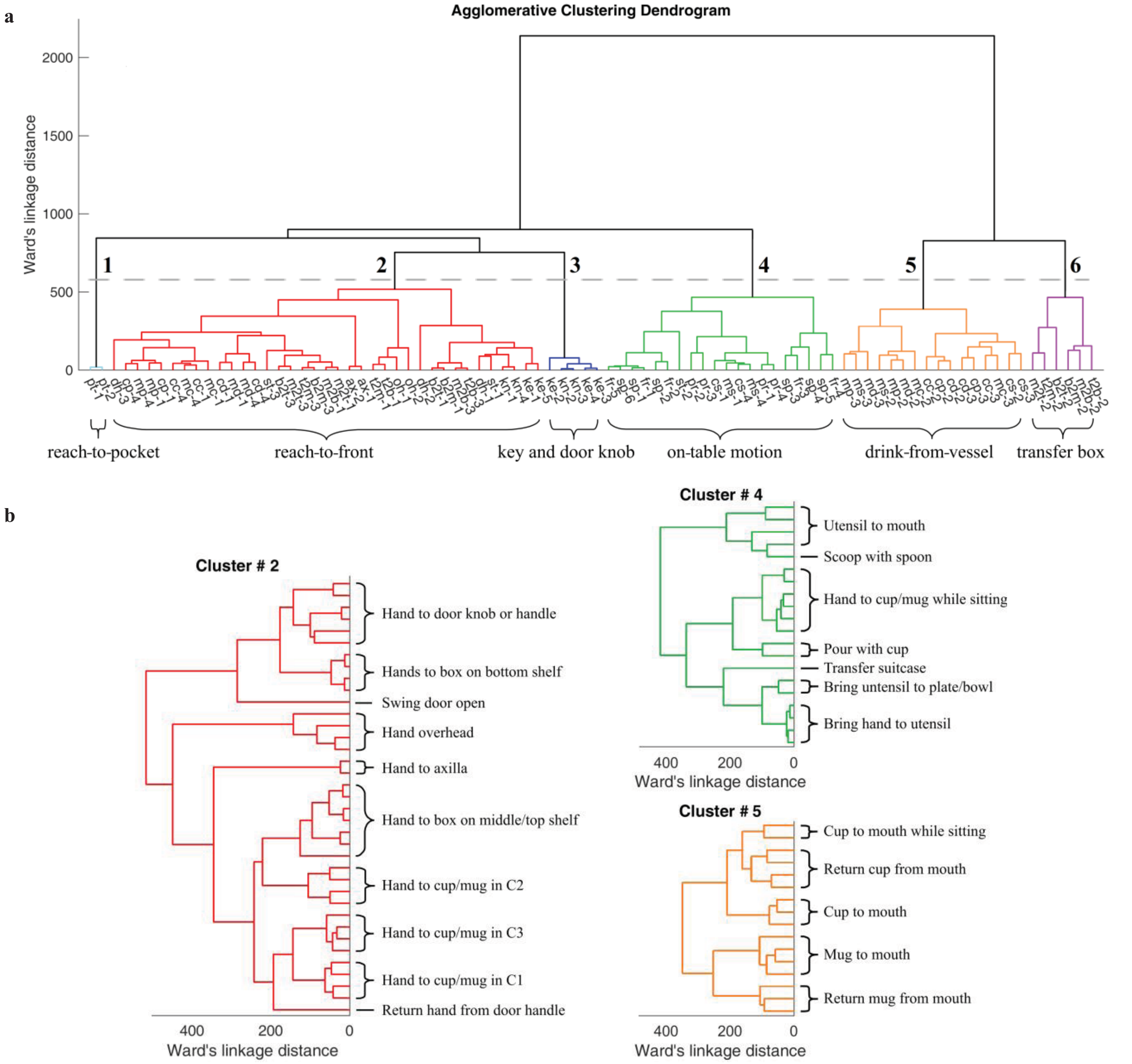

Figure 4. (a) Hierarchical clustering results, where numbers indicate the clusters. (b) A close up of the second (*reach-to-front*), fourth (*on-table motion*), and fifth (*drink-from-vessel*) clusters are shown as well.

segment from the same individual that is clustered together a score is increased by one point. The quality of clustering is then calculated by taking the score and dividing it by the maximum possible score, i.e. when the same motions belonging to the same subjects are all clustered in the same groups. It follows that a single cluster of all data gets a perfect quality score, while monotonically decreasing with an increased number of clusters. Because in total there are 86 unique motions and 5 individuals, theoretically the evaluation score could remain at 100% up to 430 clusters.

This evaluation criterion is compared against K-medoids [26], in which the number of clusters is varied from one to twenty five clusters (Fig. 5). Unlike K-means, K-medoids considers representative objects that are part of the cluster set instead of calculated centroids by identifying the median motion segments. At each iteration distances between the representative cluster object and all other motions are calculated using DTW, cluster membership is updated, and a new cluster median is found. This algorithm was performed ten times to curb local minimums.

An alternative divergence measure is also tested to verify the choice of DTW. By fitting a cubic Bezier to joint angle trajectory data, we can represent each motion segment as a set of Bezier coefficients, as has been done in [27], [28]. The feature vector is 28 elements long (4 elements for each angle). A similarity measure is obtained by calculating the Euclidean distance between motion segments. The segments are then clustered using hierarchical clustering with Ward's distance measure. Results are displayed in Fig. 5. Although possible, an optimal number of clusters was not extracted from the plot for the current analysis.

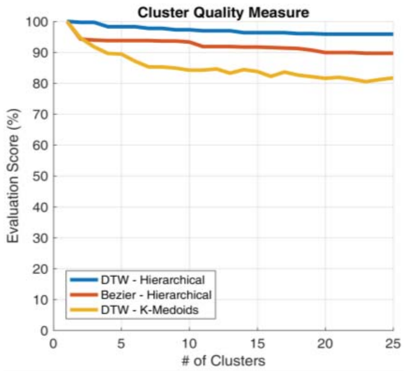

Figure 5. Quality of clustering of the two divergence measures and clustering algorithms across a range of number of clusters.

IV. DISCUSSION

Although the hierarchical tree does not output a specific number of clusters, clustered groups can be obtained by transecting the dendrogram at a desired value. The most straightforward method is using a straight line cut as is seen in Fig. 4. The location of this cut in the tree can certainly be modified to produce a different number of clusters, but for now the chosen location was easy to identify. The resulting six clusters can be summarized as follows: *reach-to-back-pocket*, *reach-to-front*, *turning a key or door knob*, *on-table motion*, *drink-from-vessel*, and *transfer-box*, suggesting that 7 DOF arm motions group largely based on start-end locations of the end effector. Prosthetists attempting to restore full ADLs capabilities to patients, and likewise rehabilitation specialists, should thus consider tasks across various end effector locations prior to tasks within any single location.

Tasks involving moving the box from one shelf to another clustered together regardless of start and end shelf locations. One explanation might be that torso motion was adjusting for the height, therefore reducing the range of motion that the arms had to travel. Similar observations can be made by noticing that cup or mug location did not significantly affect categorization. This phenomenon can be further investigated to identify the impact of torso mobility on reaching.

The divergence at which to place the dendrogram cut has been chosen heuristically, and alternative equally valid cuts can be made elsewhere. For example, by placing the cut at a divergence value of 300 the *reach-to-front* motions, the second cluster, can be subdivided into reaching to axilla, low, medium, and high elevation (Fig. 4).

The reason why the fourth cluster, *on-table motion*, contained a variety of seemingly unrelated motions was largely due to minimal arm movement. The next splitting in that cluster separated eating with a spoon or fork tasks from the rest of the motions. Because subjects would often lean over the table to imitate eating from the fork or spoon, the arm did not have to move very much and thus clustered with the other on-table motions. Since shoulder joint angles largely remained unchanged across these tasks, wrist and elbow angles played a much larger role in grouping the data within the cluster. This work can be expanded on by focusing on fewer degrees of freedom to gain insight into the wrist or wrist and elbow alone.

Cluster variability evaluation revealed that for three of the nearest pairs of motions different subjects were paired, indicating that the divergence measure captures inter-subject variability. Evaluation of the intra-cluster variability is more insightful for the larger clusters. For the *transferring a box* motions, in the sixth cluster, the furthest motion pair belong to the shortest and the tallest participants. Additionally, those motions belong to transferring a box from the bottom to the top shelf, thereby having more room for variation.

The chosen divergence measure and clustering algorithm outperformed Bezier and K-medoids methods at every number of clusters, reassuring its selection. The performance of K-medoids did not monotonically decrease with added clusters due to the algorithm reaching local minimums despite multiple iterations. Using Bezier coefficients to measure similarities between motions performed worse than DTW likely due to Bezier coefficients merely approximating the data whereas DTW takes the full joint angle data into account and calculates a more representative divergence. An evaluation score of ~95% even when evaluating 25 clusters suggests that the methodology reliably clusters like-motions.

The decision to use joint angle data as the feature vector largely relied on the ability of recorded motions to be easily interpreted across individuals as well as its low dimensional representation. However, this choice suffers from giving each joint angle an equal weight when calculating the divergence between motions, while it may have been less of an issue if Cartesian coordinates of the upper-limb segments were used instead. Additionally, proximity to the discontinuities in two of the shoulder joint angles may cause them to have an artificially larger impact when measuring motion similarity since the range of the angle is likely to be greater than the other joint angles. Alternative arm features have been proposed in the literature, such as the arm triangle [29], or defining a new angle without discontinuities [30], either of which could be used in future iterations. Finally, the decision to use a 7 DOF arm model is relevant in a variety of applications, however, the methodology can be extended to alternative models, such as to a full body kinematic chain.

V. CONCLUSION

This paper described a method that categorizes human arm motion during the performance of ADL tasks. Using DTW as a similarity measure, DBA for time-series averaging, and agglomerative hierarchical clustering with Ward's distance metric to cluster data, 6 motion categories were obtained. These clusters can be distinguished based on reaching to different locations with respect to a fixed body frame, further differentiated by types of manipulation.

The results of the described method align with intuition, making it a good candidate to describe other DOF time-series systems. The proposed approach could be applied to a subset of the presented data, such as to only the three wrist DOF, decoupling task location from wrist orientation. Verification of the method is especially important in this case since cluster results will likely be less intuitive than for the full 7-DOF arm. Future developments include identifying the average of the proposed clusters, the variance of each cluster in more detail, and the role of the torso during similar motions at different locations with respect to a fixed body frame.

REFERENCES

[1] C. J. van Andel, N. Wolterbeek, C. A. M. Doorenbosch, D. J. (H E. J.). Veeger, and J. Harlaar, “Complete 3D kinematics of upper extremity functional tasks,” *Gait Posture*, vol. 27, no. 1, pp. 120–127, 2008.

[2] T. Kang, J. He, and S. I. H. Tillery, “Determining natural arm configuration along a reaching trajectory.,” *Exp. brain Res.*, vol. 167, no. 3, pp. 352–361, 2005.

[3] M. Merad, A. Roby-Brami, and N. Jarrasse, “Towards the implementation of natural prosthetic elbow motion using upper limb joint coordination,” in *Proceedings of the IEEE RAS and EMBS International Conference on Biomedical Robotics and Biomechatronics*, 2016, pp. 821–826.

[4] R. R. Kaliki, R. Davoodi, and G. E. Loeb, “Prediction of Distal Arm Posture in 3-D Space From Shoulder Movements for Control of Upper Limb Prostheses,” *Proc. IEEE*, vol. 96, no. 7, pp. 1217–1225, 2008.

[5] L. Resnik *et al.*, “Development and Evaluation of the Activities Measure for Upper Limb Amputees,” *Arch. Phys. Med. Rehabil.*, vol. 94, no. 3, pp. 488–494, 2013.

[6] C. A. Stanger, C. Anglin, W. S. Harwin, and D. P. Romilly, “Devices for Assisting Manipulation : A Summary of User Task Priorities,” *IEEE Trans. Rehabil. Eng.*, vol. 2, no. 4, pp. 256–265, 1994.

[7] G. H. Kejlaa, “Consumer concerns and the functional value of prostheses to upper limb amputees,” *Prosthet. Orthot. Int.*, vol. 17, no. 3, pp. 157–163, 1993.

[8] F. Routhier, C. Vincent, M. J. Morissette, and L. Desaulniers, “Clinical results of an investigation of paediatric upper limb myoelectric prosthesis fitting at the Quebec Rehabilitation Institute,” *Prosthet. Orthot. Int.*, vol. 25, no. 2, pp. 119–131, 2001.

[9] A. Spiers, S. G. Khan, and G. Herrmann, *Biologically inspired control of humanoid robot arms: Robust and adaptive approaches*, 1st ed. Springer International Publishing, 2016.

[10] P. C. Doerschuk, D. E. Gustafson, and A. S. Willsky, “Upper extremity limb function discrimination using EMG signal analysis.,” *IEEE Trans. Biomed. Eng.*, vol. 30, no. 1, pp. 18–29, 1983.

[11] H.-P. Huang and C.-Y. Chen, “Development of a myoelectric discrimination system for a multi-degree prosthetic hand,” in *IEEE International Conference on Robotics and Automation*, 1999, no. 4, pp. 2392–2397.

[12] G. Averta, C. Della Santina, E. Battaglia, F. Felici, M. Bianchi, and A. Bicchi, “Unvealing the Principal Modes of Human Upper Limb Movements,” *Front. Robot. AI*, vol. 4, no. 37, pp. 1–12, 2017.

[13] D. Kulić, W. Takano, and Y. Nakamura, “Online segmentation and clustering from continuous observation of whole body motions,” *IEEE Trans. Robot.*, vol. 25, no. 5, pp. 1158–1166, 2009.

[14] D. H. Gates, L. S. Walters, J. Cowley, J. M. Wilken, and L. Resnik, “Range of Motion Requirements for Upper-Limb Activities of Daily Living,” *Am. J. Occup. Ther.*, vol. 70, no. 1, 2016.

[15] D. J. Magermans, E. K. J. Chadwick, H. E. J. Veeger, and F. C. T. van der Helm, “Requirements for upper extremity motions during activities of daily living,” *Clin. Biomech.*, vol. 20, no. 6, pp. 591–599, 2005.

[16] S. Aghabozorgi, A. Seyed, and T. Y. Wah, “Time-series clustering – A decade review,” *Inf. Syst.*, vol. 53, pp. 16–38, 2015.

[17] G. Wu *et al.*, “ISB recommendation on definitions of joint coordinate systems of various joints for the reporting of human joint motion — Part II : shoulder, elbow, wrist and hand,” *J. Biomech.*, vol. 38, no. 5, pp. 981–992, 2005.

[18] C. A. M. Doorenbosch, J. Harlaar, and D. Veeger, “The globe system: An unambiguous description of shoulder positions in daily life movements,” *J. Rehabil. Res. Dev.*, vol. 40, no. 2, p. 147, 2003.

[19] A. Fod, M. J. Mataric, and O. C. Jenkins, “Automated Derivation of Primitives for Movement Classification,” *Auton. Robots*, vol. 12, no. 1, pp. 39–54, 2002.

[20] J. Barbic, A. Safonova, J.-Y. Pan, C. Faloutsos, J. K. Hodgins, and N. S. Pollard, “Segmenting Motion Capture Data into Distinct Behaviors,” in *Proceedings of Graphics Interface*, 2004, pp. 185–194.

[21] D. Kulić, C. Ott, D. Lee, J. Ishikawa, and Y. Nakamura, “Incremental learning of full body motion primitives and their sequencing through human motion observation,” *Int. J. Rob. Res.*, vol. 31, no. 3, pp. 330–345, 2012.

[22] H. Sakoe and S. Chiba, “Dynamic Programming Algorithm Optimization for Spoken Word Recognition,” *IEEE Trans. Acoust.*, vol. 26, no. 1, pp. 43–49, 1978.

[23] F. Petitjean, A. Ketterlin, and P. Gancarksi, “A global averaging method for dynamic time warping, with applications to clustering,” *Pattern Recognit.*, vol. 44, no. 3, pp. 678–693, 2011.

[24] B. S. Everitt, S. Landau, M. Leese, and D. Stahl, *Cluster Analysis*, 5th ed. West Sussex, U.K.: John Wiley & Sons, 2011.

[25] P. Tamayo *et al.*, “Interpreting patterns of gene expression with self-organizing maps: methods and application to hematopoietic differentiation.,” *Proc. Natl. Acad. Sci. U. S. A.*, vol. 96, no. 6, pp. 2907–12, 1999.

[26] L. Kaufman and P. J. Rousseeuw, *Clustering by means of medoids*. North-Holland, 1987.

[27] O. Arikan, “Compression of Motion Capture Databases,” *ACM Trans. Graph.*, vol. 25, no. 3, pp. 890–897, 2006.

[28] J. J. Faraway, M. P. Reed, and J. Wang, “Modelling three-dimensional trajectories by using Bezier curves with application to hand motion,” *J. R. Stat. Soc. Ser. C Appl. Stat.*, vol. 56, no. 5, pp. 571–585, 2007.

[29] C. Fang and X. Ding, “A Set of Basic Movement Primitives for Anthropomorphic Arms,” in *IEEE International Conference on Mechatronics and Automation*, 2013, pp. 639–644.

[30] T. Masuda, A. Ishida, L. Cao, and S. Morita, “A proposal for a new definition of the axial rotation angle of the shoulder joint,” *J. Electromyogr. Kinesiol.*, vol. 18, no. 1, pp. 154–159, 2008.